A SoH Diagnosis and Prognosis Method to Identify and Quantify Degradation Modes in Li-ion Batteries using the IC/DV technique

C. Pastor-Fernández, W.D. Widanage*, G.H. Chouchelamane †, J. Marco**

**WMG, University of Warwick, United Kingdom,*
c.pastor-fernandez@warwick.ac.uk, dhammika.widanalage@warwick.ac.uk, james.marco@warwick.ac.uk
†Jaguar Land Rover, United Kingdom, gchouch1@jaguarlandrover.com

Keywords: Lithium-ion batteries, Battery Management System, Degradation modes, IC/DV technique, SoH diagnosis and prognosis.

Abstract

Accurate State of Health (SoH) diagnosis and prognosis of Lithium-ion batteries (LIBs) may become an important estimate for the Battery Management System (BMS) if it can be acted upon to de-rate the demands placed on the battery in order to reduce the rate of ageing and to extend battery life. The BMS often quantifies SoH based on capacity (SoH_E) and power fade (SoH_P) without diagnosing the root causes. In line with this, Incremental Capacity (IC) and Differential Voltage (DV) techniques are used to identify and quantify degradation modes as well as to estimate and to predict the SoH_E. These techniques were applied to four parallelised LIBs loaded with a constant current profile for 500 cycles. Loss of active material and loss of lithium ions were identified to be the most relevant degradation modes for this experiment. Moreover, a linear relationship between the intensity of the peaks of the IC and DV curves were identified with respect to the SoH_E. This result may enable the future estimation and prediction of SoH_E in a simple way. Overall, the outcomes of this work may support novel strategies to control SoH_E within the BMS, so that the rate of battery degradation can be reduced.

1 Introduction

Control of lithium-ion batteries is required to mitigate the effects of cell ageing. Despite this, SoH diagnosis and prognosis functions have not been effectively implemented in commercial Battery Management Systems (BMS) yet [1].

SoH is defined as the capability of a battery to store energy (SoH_E) or deliver power (SoH_P) relative to its initial conditions. SoH is often quantified in terms of the decrease in cell capacity (SoH_E) and the increase in cell resistance (SoH_P) [1]. The limits of the SoH are Begin of Life (BoL) and End of Life (EoL) values. BoL (SoH=100%) represents the state when the battery is new, and EoL (SoH=0%) is defined as the condition when the battery cannot meet the performance specification for the particular application for which it was designed [2]. For automotive applications, the EoL has been defined in previous publications [1], [2] and procedures [3], [4] and are provided in Equation (1) and Equation (2):

$$C_{EoL} = 0.8 \cdot C_{BoL} \tag{1}$$

$$R_{EoL} = 2 \cdot R_{BoL} \tag{2}$$

SoH_E and SoH_P are often calculated as a percentage with respect to the difference between BoL and EoL in either capacity (Equation (3)) or resistance (Equation (4)) [2].

$$SoH_E = \frac{C - C_{EoL}}{C_{BoL} - C_{EoL}} \cdot 100 \tag{3}$$

$$SoH_P = \frac{R - R_{EoL}}{R_{BoL} - R_{EoL}} \cdot 100 \tag{4}$$

These metrics are directly related to vehicle level attributes that limit driving range and vehicle power respectively. These metrics do not however provide any insights into the root causes of battery degradation [5]. This knowledge will ultimately support lifetime control strategies that aim to maintain the vehicle performance and to maximise battery lifespan. Root causes of battery degradation are commonly categorised in: conductivity losses (CL); Loss of Active Material (LAM); or, Loss of Lithium-Inventory (LLI), as Figure 1C) illustrated [6].

There are several diagnosis techniques such as Electrochemical Impedance Spectroscopy, Slow Rate Cyclic Voltammetry, Differential Thermal Voltammetry, Incremental Capacity (IC) and Differential Voltage (DV) which could identify and quantify degradation modes in real-time applications and could be suitable for implementation within the BMS. After analysing each of these methods it was concluded that the most promising diagnosis tools are IC and DV [1], [5]–[10] because they can encompass the identification and quantification of degradation modes as well as SoH diagnosis and prognosis. IC and DV techniques were applied in this study to identify and quantify degradation modes and to diagnose and prognose SoH of four parallelised Lithium-ion Batteries (LIBs) cycled with a constant driving profile for 500 charge-discharge cycles.

The structure of this paper is as follows: Section 2 provides an introduction of the IC and DV techniques, describing the methodology and metrics employed to identify and quantify the degradation modes, Section 3 summarises the experimental investigation conducted for this work, Section 4 presents the

results obtained, Section 5 outlines the limitations of this approach and areas that could be further investigated and finally Section 6 draws the main conclusions of this study.

2 Methodology

2.1 Incremental capacity and differential voltage technique

IC/DV technique consists of calculating the rate of change of electrochemical equilibrium phase (EEP) changes. EEP changes are defined as the process of intercalation and de-intercalation of Li-ions between the electrodes. These processes can be quantified when the system is in equilibrium. Figure 1A) and B) illustrate that the constant gradient regions in the pseudo-Open Circuit Voltage (OCV) curve are related to EEP changes, which manifests themselves as peaks in the IC curves or valleys in the DV curves. The magnitude of the peaks/valleys changes with respect to voltage or capacity (IC and DV, respectively), depending on the cell chemistry [5] and ageing conditions, e.g. average temperature, C-rate, average state of charge (SoC) and depth of discharge difference (ΔDoD) [7].

IC and DV methods provides similar information, IC uses the pseudo-OCV curve to asses battery ageing, whereas DV uses cell capacity. The IC curve is derived by differentiating the battery charge Q with respect to the terminal voltage V (for a positively or negatively polarised electrode). Mathematically, the IC curve was computed as the gradient of Q with respect to V using Equation (1):

$$\frac{dQ}{dV} \approx \frac{\Delta Q}{\Delta V} \tag{1}$$

Calculating the inverse of the IC curve yields the DV curve. Mathematically, the DV curve is derived as the gradient of V with respect to Q using Equation (2):

$$\frac{dV}{dQ} \approx \frac{\Delta V}{\Delta Q} \tag{2}$$

In both cases the gradient function from MATLAB [11] was employed to perform these calculations. The measurements of the charge Q and the terminal voltage V are often disturbed by noise. To reduce the amount of noise in the measurements the IC and DV curves are smoothed and thus, the derivatives of the curves will be improved. The smoothing procedure consists firstly of averaging OCV values which are related to any repeated capacity measurements, and secondly interpolating the remaining data points equally. Despite the fact that IC and DV curves are related, both curves are often employed, since the information they provide is complimentary and when combined yields greater insights into the rate and nature of the degradation within the cell.

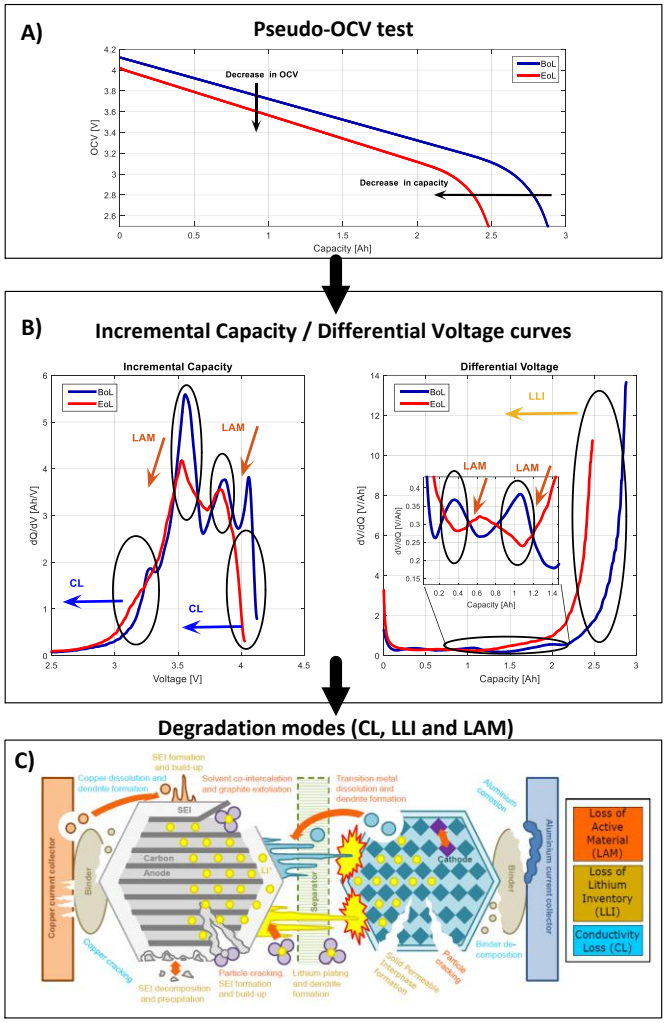

Figure 1: Relationship between A) pseudo-OCV data, B) IC and DV curves and C) degradation modes (bottom figure adapted from [12]).

2.2 Identification of degradation modes

To identify and quantify degradation modes this work follows the guidelines proposed in [6]. This work has been supported by other authors in the past few years [5], [8], [13] because it relates the IC/DV curves with the most pertinent degradation modes in a simple way. IC/DV curves are derived from half-cell measurements in [6]. Half-cell measurements allow each degradation mode to be associated with respect to the electrode where they occur. For this case, full-cell measurements were used to analyse the IC/DV curves in a similar way as was done in [6] without relating the degradation modes with the electrodes where they occur. As an advantage, full-cell measurements emulates the same conditions as the cells are subjected in a battery pack, making this technique potentially implementable into a BMS.

Figure 1B) shows the changes in the IC/DV curves with respect to the degradation modes. In general, four changes are identified: shifting to lower voltages (IC), reduction of the

magnitude of the peaks (IC), reduction of the valleys (DV) and shifting to lower capacities (DV) [6].
According to [6], shifting to lower voltages (IC) is linked to CL, reduction of the intensity of the peaks (IC and DV) is related to LAM, and shifting to lower capacities (DV) to LLI. Table 1 relates the change of the IC/DV curves with the corresponding degradation modes and ageing mechanisms.

CL is related to shifting toward lower voltages in the IC curve. According to Ohm's law [5], [8], [13], the battery terminal voltage is often computed as the OCV minus the voltage drop due to the ohmic resistance. The decrease of the OCV in the IC curve with cycle number is then related to the increase of the ohmic resistance. This increase in resistance is commonly related to CL [14].
Shifting toward lower capacities in the DV curve is linked to LLI. The OCV curve relates the change of the OCV to the capacity and the SoC. As long as the cell is aged, the OCV and the available capacity decrease. From an electrochemical viewpoint, the reduction of the OCV is translated into a decrease of the available number of Li-ions [6], [15].

Change in IC/DV curves	*Unit*	*Degradation mode*	*Ageing mechanism*
Change in IC curve: shift to lower voltages	[V]	CL	Copper dissolution and dendrite formation. Copper cracking and contact loss. Aluminium corrosion and contact loss. Binder decomposition and contact loss. Structural disordering.
Change in DV curve: shift to lower capacities	[Ah]	LLI	SEI formation and build-up. SEI decomposition and precipitation. Solid permeable interphase formation. Particle cracking, pore clogging and particle disconnection.
Change in IC curve: decrease of magnitude of the peaks	[Ah/V]	LAM	Solvent co-intercalation and graphite exfoliation. Transition metal dissolution and dendrite formation. Structural disordering.
Change in DV curve: decrease of valleys	[V/Ah]		

Table 1: Relationship between changes in IC/DV curves, degradation modes and ageing mechanisms.

Reduction of the magnitude of the peaks in the IC curve and shifting to lower voltages represents a reduction of the capacity at a particular potential. Similarly, reduction of the local peaks in the valleys in the DV curve and shifting to lower capacities represents a reduction of the voltage phase change at a particular capacity. For both cases, the voltage and capacity phase change slightly, and so implies the system is close to equilibrium and therefore the total overpotential is almost zero. From the electrochemical viewpoint, these phase changes are attributed to structure disordering of the active materials (LAM) due to mechanical stress during cycling [5], [8], [13]. Similarly for the LLI, this means that the graphite could not be lithiated to the same level as it had been initially [6], [8].

An increase in the intensity of the peaks in the IC curve and shifting to higher voltages, or an increase in the valleys in the DV curve and shifting to higher capacities could also occur. The increase in voltage and capacity are related to the reversible phenomenon whereby electrode and electrolyte particles are reformed [16].

2.3 Quantification of degradation modes

Previous studies [6], [7] quantify degradation modes using IC/DV based on capacity loss. In order to compare the results of this study with previous literature [9], the growth of each degradation mode from the changes of the IC/DV curves is calculated.

According to Table 1 the growth of degradation (*Gdeg*) of each degradation mode for each characterisation test is computed using Equation (3), Equation (4) and Equation (5) as a function of *OCV*, capacity *C* and $\frac{\Delta Q}{\Delta V}$ values:

$$CL_k(\%) = \frac{\max(OCV)_1 - \max(OCV)_k}{\max(OCV)_1} \cdot 100 \quad (3)$$

$$LAM_k(\%) = \frac{\max(C)_1 - \max(C)_k}{\max(C)_1} \cdot 100 \quad (4)$$

$$LLI_k(\%) = \frac{\max\left(\frac{\Delta Q}{\Delta V}\right)_1 - \max\left(\frac{\Delta Q}{\Delta V}\right)_k}{\max\left(\frac{\Delta Q}{\Delta V}\right)_1} \cdot 100 \quad (5)$$

For k=1…11

For this experimental case, it was observed that the decrease of the magnitude of the local peaks in the DV curve was not as clear as in the case of the peaks in the IC curves, and so from here on the DV curves were no longer considered to quantify LAM.

3 Experimental investigation

Four Nickel Cobalt Aluminium (NCA) Li-ion cells connected in parallel were cycled to generate the pseudo-OCV data

required to derive the IC/DV curves. The cells were initially aged by 0, 50, 100 and 150 cycles respectively before being connected in parallel and so an SoH imbalanced parallel combination was created. The parallel cells then underwent 500 cycles until their C_{EoL} was reached (refer to Equation (1)). To simplify the analysis and discussion, this paper only focuses on studying the least aged cell. The cells were aged at a constant temperature of 25 °C ±1 °C. The cycle profile was composed of Constant-Current (CC) Constant-Voltage (CV) charging protocol followed by 1C discharge until the lower voltage limit was reached (2.5 V). The CC phase involved charging the cell at C/2 until the end of charge voltage was reached (4.2 V). The CV phase then consisted of charging the cell until the current reduced to C/20 (150mA). Every 50 cycles the cells were individually characterised using the pseudo-OCV test. The pseudo-OCV test consisted of charging the cells to the higher voltage limit (100% SoC) according to the CC-CV protocol followed by discharging the cells at C/10 to the lower voltage limit (0% SoC). The cell's capacity was then defined as the charge dissipated over this discharge event (refer to Figure 1A)).

4 Results

4.1 Identification of degradation modes

Figure 2A) and B) illustrate the IC and DV curves derived for 0, 250 and 500 cycles.

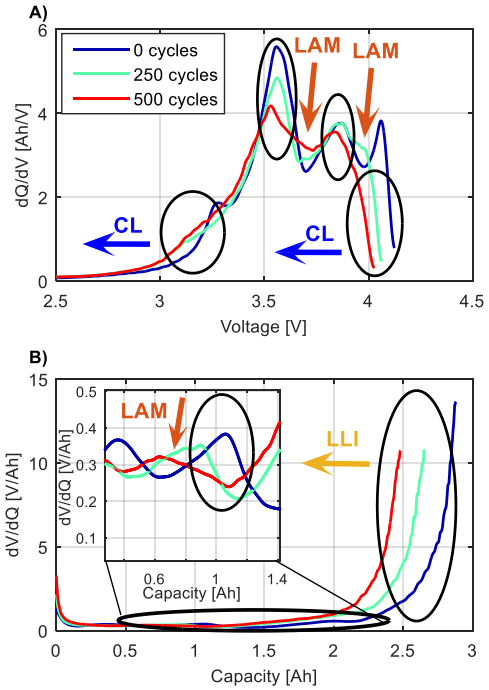

Figure 2: Identification of degradation modes for 0, 250 and 500 cycles based on A) IC and B) DV curves.

Figure 2A) shows that the IC curves are shifting to the left with cycle number due to CL and that the magnitude of the peaks are decreasing due to LAM. It can be seen that for the first half of the experiment the intensity of the peaks decreases more than for the last half of the experiment, indicating that the rate of change of LAM is not constant throughout the experiment. Figure 2B) shows that the capacity decreases over cycle number due to the reduction of the concentration of Li-ions, which according to Section 2.2 is representative of LLI [6]. Similarly as for the IC curve, LAM can also be identified through the DV curves as the reduction of the magnitude of the local peaks in the valleys.

4.2 Quantification of degradation modes

Using Equation (3), Equation (4) and Equation (5) the growth in percentage of each degradation mode is computed over cycle number. Figure 3 illustrates that LAM and LLI grows exponentially over cycle number from 0% to 25% and from 0% to 15%, respectively. The growth of CL with respect to LAM and LLI is significantly lower (from 0% to 3%) showing that CL is less relevant in this experiment. This result is in agreement with [17], where is claimed that manufacturing processes in commercial Li-ion cells largely eliminate the degradation effects attributed to CL.

Dubarry et al. [9] applied the IC/DV technique to a similar type of chemistry and testing scenario. The contribution of each degradation mode as capacity fade percentage was computed and they concluded that LAM and LLI were the most pertinent degradation modes, increasing exponentially with respect to cycle number. This conclusion agrees with the results presented here.

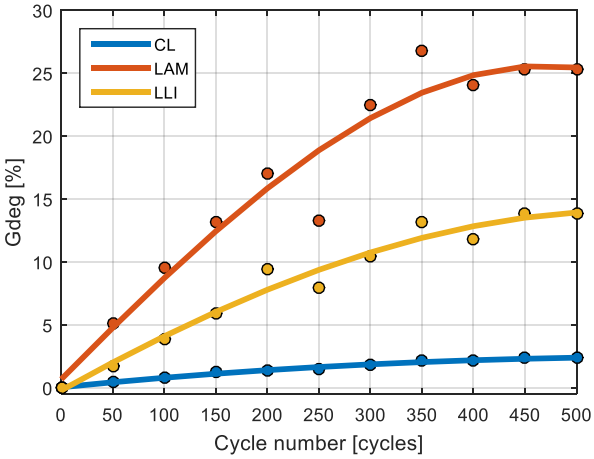

Figure 3: Growth of degradation (Gdeg) of each degradation mode over cycle number.

4.3 SoH diagnosis and prognosis

Apart from identifying and quantifying degradation modes, IC/DV can also be used to estimate (diagnose) the current SoH and to predict (prognose) the future SoH.

The charge accumulated over the C/10 discharge event of the pseudo-OCV test (refer to Section 3) was employed to compute the SoH_E using Equation (1). Figure 4A) illustrates the SoH_E over cycle number. It highlights that the SoH_E decreases faster

for the first half of the experiment than for the second half of the experiment. This result outlines that speed of degradation changes despite the testing conditions being kept constant throughout the experiment. From 400 to 500 cycles is also observed that SoH_E increases, which may be explained due to capacity reversible effects.

Previous work [1], [10] showed that a linear SoH_E estimation can be derived from further analysis of IC/DV curves. This linear relationship consists of obtaining a correlation between the SoH_E and the peaks of the IC curves (refer to Figure 2A)), or the SoH_E with the local peaks of the valleys of the DV curves (refer to Figure 2B)).

Figure 4B) illustrates the linear relationship of the highest peak of the IC curve with respect to SoH_E. The adjusted R^2 value of this fitted line is 0.9549 indicating that the line relates strongly the variability of the response data with respect to its mean. The magnitude of the peak decreases over cycle number as indicated in Figure 2A). Likewise, Figure 4C) relates the highest peak of the valley of the DV curve with SoH_E. The intensity of the peak also decreases upon cycling. However the resulting fitted line has an adjusted R^2 value of 0.4534, highlighting that DV peaks cannot be linearly fitted with respect to SoH_E with the same level of accuracy as the case of the IC peaks. This is also analysed in [1], where they fitted the DV peaks to a power law. As IC and DV peaks are employed with the same aim, it would be recommended to use the IC peaks since their relationship with SoH_E fits linearly better than the DV peaks.

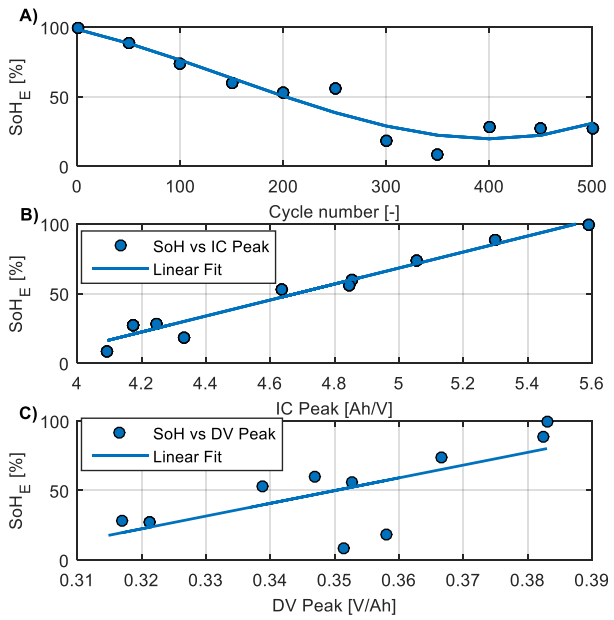

Figure 4: A) SoH_E over number of cycles, B) SoH_E vs peaks of the IC curves approximated by a linear fit and C) Linear relationship between SoH_E vs peaks of the valleys in the DV curves.

For both cases the linear relationship suggests the possibility to simply estimate SoH_E by measuring the intensity of the peaks in the IC and DV curves. This linear relationship could also enable SoH_E prognosis to estimate the remaining life of the cell. The authors ascertain that measuring the magnitude of the peaks is feasibly implemented into a modern BMS and this approach is therefore suitable for future commercial applications.

5 Limitations of this study and further work

The degradation modes identified with the IC/DV curves could be compared using post-mortem analysis. This electrochemical analysis can identify more confidently the degradation modes in LIBs.

The linear relationship between SoH_E and the intensity of the peaks in the IC/DV curves need to be validated under different operating modes (e.g. cycling and storage) and conditions (e.g. temperature, SoC, ΔDoD or C-rates) which commercial Li-ion batteries may be subject to. After such validation, this technique could be embedded in a BMS so that the main causes of battery ageing (LAM, LLI or CL) could be identified. However, the embedded implementation of this technique has the limitation of performing the pseudo-OCV test since such a test requires low dynamic operation. Thus, a possibility to perform this test could be in the situation when the vehicle is on service. Instead of performing the pseudo-OCV test, recent studies suggested to predict the pseudo-OCV curve based on estimator algorithms such as support vector machine [10] or extended Kalman filter [18].

Identification and quantification of degradation modes add information to improve SoH diagnosis and prognosis functions within the BMS. The next step is to determine how the BMS will use such information, as a part of a control strategy, to mitigate ageing mechanism effects.

6 Conclusions

Based on Li-ion pseudo-OCV measurements at full-cell level, this study proposes a method to identify and quantify degradation modes using IC/DV curves. It was demonstrated that LAM and LLI represent the most pertinent degradation modes for this experiment. Furthermore, the magnitude of the peaks in IC/DV curves were linearly dependent on the decrease of SoH_E over cycle number. This linear relationship will allow the BMS to estimate the change of SoH_E in a simple way, which may be further investigated in the future for real-time battery diagnosis and prognosis. Identification and quantification of degradation modes and SoH_E diagnosis and prognosis using IC/DV curves could be implemented in the future within the BMS for commercial applications. This approach will allow the BMS to pre-empt battery failures during normal operation.

Acknowledgements

The research presented within this paper is supported by the Engineering and Physical Science Research Council (EPSRC - EP/ I01585X/1) through the Engineering Doctoral Centre in High Value, Low Environmental Impact Manufacturing. The

research was undertaken with the WMG Centre High Value Manufacturing Catapult (funded by Innovate UK) in collaboration with Jaguar Land Rover. The authors would like to thank Dr. Mark Tucker, Dr. Kotub Uddin and Thomas Bruen for their support on the experimental measurements and analysis of the results.

References

[1] M. Berecibar, N. Omar, and M. Garmendia, "SOH estimation and prediction for NMC cells based on degradation mechanism detection," 2015.

[2] D. Andre, C. Appel, T. Soczka-Guth, and D. U. Sauer, "Advanced mathematical methods of SOC and SOH estimation for lithium-ion batteries," *J. Power Sources*, vol. 224, no. 0, pp. 20–27, 2013.

[3] G. Hunt, "Electric Vehicle Battery Test Procedures - Rev. 2," *United States Adv. Batter. Consort.*, no. January, 1996.

[4] R. 0 INL/EXT-07e12536, "Battery Test Manual for Plug-in Hybrid Electric Vehicles," 2008.

[5] X. Han, M. Ouyang, L. Lu, J. Li, Y. Zheng, and Z. Li, "A comparative study of commercial lithium ion battery cycle life in electrical vehicle: Aging mechanism identification," *J. Power Sources*, vol. 251, pp. 38–54, Apr. 2014.

[6] M. Dubarry, C. Truchot, and B. Y. Liaw, "Synthesize battery degradation modes via a diagnostic and prognostic model," *J. Power Sources*, vol. 219, pp. 204–216, 2012.

[7] M. Dubarry, B. Y. Liaw, M.-S. Chen, S.-S. Chyan, K.-C. Han, W.-T. Sie, and S.-H. Wu, "Identifying battery aging mechanisms in large format Li ion cells," *J. Power Sources*, vol. 196, no. 7, pp. 3420–3425, Apr. 2011.

[8] E. Sarasketa-Zabala, F. Aguesse, I. Villarreal, L. M. Rodriguez-Martinez, C. M. López, and P. Kubiak, "Understanding Lithium Inventory Loss and Sudden Performance Fade in Cylindrical Cells during Cycling with Deep-Discharge Steps," *J. Phys. Chem. C*, vol. 119, no. 2, pp. 896–906, 2015.

[9] M. Dubarry, C. Truchot, B. Y. Liaw, K. Gering, S. Sazhin, D. Jamison, and C. Michelbacher, "Evaluation of commercial lithium-ion cells based on composite positive electrode for plug-in hybrid electric vehicle applications. Part II. Degradation mechanism under 2C cycle aging," *J. Power Sources*, vol. 196, no. 23, pp. 10336–10343, Dec. 2011.

[10] C. Weng, Y. Cui, J. Sun, and H. Peng, "On-board state of health monitoring of lithium-ion batteries using incremental capacity analysis with support vector regression," *J. Power Sources*, vol. 235, pp. 36–44, Aug. 2013.

[11] The Mathworks Inc., "corrcoef," 2015. [Online]. Available: http://uk.mathworks.com/help/matlab/ref/corrcoef.html. [Accessed: 25-Apr-2016].

[12] C. R. Birkl, "Degradation mechanisms." [Online]. Available: http://epg.eng.ox.ac.uk/sites/default/files/Christoph/Degradation_mechanisms_cChristoph_Birkl_small.png. [Accessed: 12-Jan-2016].

[13] H. M. Dahn, A. J. Smith, J. C. Burns, D. A. Stevens, and J. R. Dahn, "User-Friendly Differential Voltage Analysis Freeware for the Analysis of Degradation Mechanisms in Li-Ion Batteries," *J. Electrochem. Soc.* , vol. 159 , no. 9 , pp. A1405–A1409, Jan. 2012.

[14] D. P. Abraham, S. D. Poppen, A. N. Jansen, J. Liu, and D. W. Dees, "Application of a lithium–tin reference electrode to determine electrode contributions to impedance rise in high-power lithium-ion cells," *Electrochim. Acta*, vol. 49, no. 26, pp. 4763–4775, Oct. 2004.

[15] M. Dubarry, V. Svoboda, R. Hwu, and B. Yann Liaw, "Incremental Capacity Analysis and Close-to-Equilibrium OCV Measurements to Quantify Capacity Fade in Commercial Rechargeable Lithium Batteries," *Electrochem. Solid-State Lett.*, vol. 9, no. 10, pp. A454–A457, 2006.

[16] A. J. Smith, J. C. Burns, D. Xiong, and J. R. Dahn, "Interpreting High Precision Coulometry Results on Li-ion Cells," *J. Electrochem. Soc.*, vol. 158, no. 10, pp. A1136–A1142, 2011.

[17] J. W. Braithwaite, A. Gonzales, G. Nagasubramanian, S. J. Lucero, D. E. Peebles, J. A. Ohlhausen, and W. R. Cieslak, "Corrosion of Lithium-Ion Battery Current Collectors," *J. Electrochem. Soc.*, vol. 146, no. 2, pp. 448–456, 1999.

[18] S. Tong, M. P. Klein, and J. W. Park, "On-line optimization of battery open circuit voltage for improved state-of-charge and state-of-health estimation," *J. Power Sources*, vol. 293, pp. 416–428, Oct. 2015.